J|A|C|S
ARTICLES
Published on Web 04/19/2003

Comparison of Formation of Reactive Conformers (NACs) for the Claisen Rearrangement of Chorismate to Prephenate in Water and in the *E. coli* Mutase: The Efficiency of the Enzyme Catalysis

Sun Hur and Thomas C. Bruice*

Contribution from the Department of Chemistry and Biochemistry, University of California at Santa Barbara, Santa Barbara California, 93106

Received August 8, 2002; Revised Manuscript Received January 3, 2003; E-mail: tcbruice@chem.ucsb.edu

Abstract: The Claisen rearrangements of chorismate (CHOR) in water and at the active site of *E. coli* chorismate mutase (EcCM) have been compared. From a total of 33 ns molecular dynamics simulation of chorismate in water solvent, seven diaxial conformers **I**−**VII** were identified. Most of the time (∼99%), the side chain carboxylate of the chorismate is positioned away from the ring due to the electrostatic repulsion from the carboxylate in the ring. Proximity of the two carboxylates, as seen in conformer **I**, is a requirement for the formation of a near attack conformer (NAC) that can proceed to the transition state (TS). In the EcCM·CHOR complex, the two carboxylates of CHOR are tightly held by Arg28 of one subunit and Arg11* of the other subunit, resulting in the side chain C16 being positioned adjacent to C5 with their motions restricted by van der Waals contacts with methyl groups of Val35 and Ile81. With the definition of NAC as the C5···C16 distance ≤3.7 Å and the attack angle ≤30°, it was estimated from our MD trajectories that the free energy of NAC formation is ∼8.4 kcal/mol above the total ground state in water, whereas in the enzyme it is only 0.6 kcal/mol above the average of the Michaelis complex EcCM·CHOR. The experimentally measured difference in the activation free energies of the water and enzymatic reactions ($\Delta\Delta G^{\ddagger}$) is 9 kcal/mol. It follows that the efficiency of formation of NAC (7.8 kcal/mol) at the active site provides ∼90% of the kinetic advantage of the enzymatic reaction as compared to the water reaction. Comparison of the EcCM·TSA (transition state analogue) and EcCM·NAC simulations suggests that the experimentally measured 100 fold tighter binding of TSA compared to CHOR does not originate from the difference between NAC and the TS binding affinities, but might be due to the free energy cost to bring the two carboxylates of CHOR together to interact with Arg28 and Arg11* at the active site. The two carboxylates of TSA are fixed by a bicyclic structure. The remaining ∼10% of $\Delta\Delta G^{\ddagger}$ may be attributed to a preferential interaction of Lys39−NH_3^+ with O13 ether oxygen in the TS.

Introduction

We have been interested in the importance of ground state conformations in determining the rate enhancements of enzymatic reactions. The rate enhancement of an enzymatic reaction is generally defined in terms of the first-order rate constant for the enzymatic reaction (k_{cat}) compared to the pseudo-first-order rate constant of the nonenzymatic reaction (k_{non}) in water at neutrality. We have chosen to examine one-substrate reactions which involve intramolecular rearrangements of substrates without the formation of enzyme−substrate covalent intermediates. These features make it feasible to directly compare reactions in both water and enzyme. We describe here the pericyclic rearrangement (Chart 1) of chorismate (CHOR) to prephenate in water and when catalyzed by *E. coli* chorismate mutase (EcCM). It has been experimentally determined for this reaction that $k_{cat}/k_{non} = 10^6$.[1]

NACs are defined as conformers in which reacting atoms are at van der Waals distance and the angle of approach is ±15° of the angle of the bond forming in the transition state (TS). For the chorismate → prephenate reaction, the criteria for NAC are the C5···C16 distance ≤3.7 Å and the attack angle ≤30° (Chart 1). NACs are turnstiles that reactants must pass through in order to reach the TS. In the reactions of monoester carboxylic acids to form cyclic anhydrides, the value of $\Delta G^{\ddagger}$ is a linear function of the log of the mole fraction of conformers of a particular reactant being NAC.[2] Menger has determined the rate constants of pericyclic rearrangements much like chorismate → prephenate reaction. He has shown that the rate of reaction is related to the distance between the reacting moieties.[3] In this pericyclic rearrangement model systems and the earlier ring closure of monoesters, the crucial factor for determining a relative rate constant is the population of reactive conformers (NACs) in the ground state. It has been proposed that this "ground-state effect" has no counterpart in enzymatic reactions. There is no experimental evidence for this statement. The present

(1) Ganem, B. *Angew. Chem., Int. Ed. Engl.* **1996**, *35*, 937−945.

(2) Lightstone, F. C.; Bruice, T. C. *J. Am. Chem. Soc.* **1996**, *118*, 2595−2605.

(3) Khanjin, N. A.; Snyder, J. P.; Menger, F. M. *J. Am. Chem. Soc.* **1999**, *121*, 11 831−11 846.

10.1021/ja0210648 CCC: $25.00

Chart 1

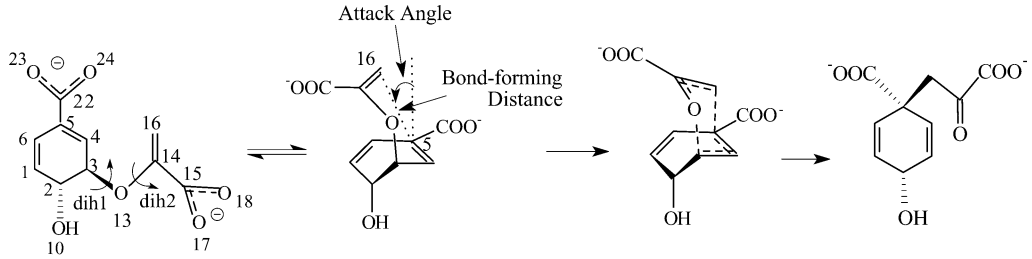

Chart 2

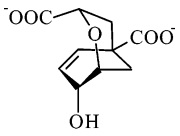

TSA

study establishes that the population of the reactive conformers (NACs) is of overwhelming importance in explaining the rate enhancement by *E. coli* chorismate mutase.

The design and synthesis of the transition state analogue (TSA, Chart 2) for chorismate mutase by Paul Bartlett has been of historical importance in the support of the proposal that in the enzymatic reaction the transition state is held more tightly than is the ground state.[4] In the present study, we compare the molecular dynamic structures of the *E. coli* enzyme in aqueous solution when bound with NAC, transition state (TS) and TSA.

Methods

MD Simulation of Chorismate in Water. A molecular dynamics (MD) simulation of a chorismate molecule in a pool of water was carried out using the program CHARMM (version 25b2).[5] The force fields of chorismate was taken from the parameters that have been calculated in our previous study[6] at the MP2/aug-cc-pVDZ//B3LYP/6-31+G(d,p) level of theory using Gaussian98.[7] A molecule of chorismate, with both carboxyl groups ionized, was placed in a TIP3P[8] water box of dimension 24 × 24 × 24 Å^3. The system was energy-minimized using a combination of steepest descent (SD) and adopted basis Newton−Raphson (ABNR) methods.[5] An MD simulation was performed on the energy-minimized system. A periodic boundary condition was used to simulate a continuous water pool. The SHAKE algorithm was used to constrain bonds containing hydrogens to their equilibrium lengths.[9] The Verlet leapfrog algorithm was used to integrate the equations of motion.[10] A time step of 1.5 fs was used and the nonbonded list was updated every 20 time steps. The nonbonded interactions were cut off at 12 Å. The Coulombic term was cut off using a force shifting function and the Lennard-Jones term was cut off with a switching function. The system was initially coupled to a 200 K heat bath for 15 ps using a coupling constant of 5 s^{-1}. The system was subsequently coupled to a heat bath at 300 K for the rest of the simulation using a coupling constant of 5 s^{-1}. The pressure was constantly maintained by a Berendsen algorithm using an isothermal compressibility of 4.63 × 10^{-5} atm^{-1} and a pressure coupling constant of 5.0 ps.[11] Coordinates were saved every 100 time steps. The final system contains one chorismate molecule and 395 TIP3P water molecules.

The relative population of chorismate conformer was obtained from the total time fraction of chorismate remaining in each conformation during the MD simulation. To compensate for any influence of initial geometry in obtaining a meaningful probability for the presence of each conformer, ten MD simulations were initiated from 10 different initial geometries. These geometries differed by rotating the side chain dihedral angle 1 (dih1: C4−C3−O13−C14) from 0°−360°. Only two simulations, one started from dih1 = 40° and the other started from dih1 = 60°, were continued because, after the system reached equilibrium, the resultant structures of all the other simulations were similar to either of these two. The simulation started from dih1 = 40° was continued up to 10 ns, after which all the kinetic energy of the system gradually began to be converted into a translational energy. This phenomenon, known as "the flying ice cube", is one pathological form of the problem in using the standard MD protocol to maintain the constant temperature when the simulation is continued for a long period.[12] To avoid this problem, another simulation started from dih1 = 60° was performed with one atom (C5) fixed at a position. The simulation was continued for 20 ns when any evidence of the flying ice cube was not found. The latter simulation showed similar thermodynamic and kinetic behaviors of chorismate as in the former simulation. Comparison of two simulations suggested that both systems search similar conformational space after 1 ns despite starting from different geometries.

Calculation of the First-order Rate Constant for Disappearance of Each Conformer. In the 30 ns MD trajectories described above, seven conformers **I**−**VII** were identified (Figure 1). Conformers **II**−**V** occur most frequently (about 16 times). Each time they formed, the time period of chorismate remaining in that conformation (lifetime[13]) was recorded. The statistics of the lifetime for each conformer was used to create a plot of log(population) vs lifetime (Figure 2). The linear fit for each plot has a correlation coefficient greater than 0.95. This

(4) Bartlett, P. A.; Nakagawa, Y.; Johnson, C. R.; Reich, S. H.; Luis, A. *J. Org. Chem.* **1988**, *53*, 3195−3210.
(5) Brooks, B. R.; Bruccoleri, R. E.; Olafson, B. D.; States, D. J.; Swaminathan, S.; Karplus, M. *J. Comput. Chem* **1983**, *4*, 187−217.
(6) Hur, S.; Bruice, T. C. *Prot. Natl. Acad. Sci. U.S.A.* **2002**, *99*, 1176−1181.
(7) Frisch, M. J.; Trucks, G. W.; Schlegel, H. B.; Scuseria, G. E.; Robb, M. A.; Cheeseman, J. R.; Zakrzewski, V. G.; Montgomery, J. A.; Stratmann, R. E.; Burant, J. C.; Dapprich, S.; Millam, J. M.; Daniels, A. D.; Kudin, K. N.; Strain, M. C.; Farkas, O.; Tomasi, J.; Barone, V.; Cossi, M.; Cammi, R.; Mennucci, B.; Pomelli, C.; Adamo, C.; Clifford, S.; Ochterski, J.; Petersson, G. A.; Ayala, P. Y.; Cui, Q.; Morokuma, K.; Malick, D. K.; Rabuck, A. D.; Raghavachari, K.; Foresman, J. B.; Cioslowski, J.; Ortiz, J. V.; Stefanov, B. B.; Liu, G.; Liashenko, A.; Piskorz, P.; Komaromi, I.; Gomperts, R.; Martin, R. L.; Fox, D. J.; Keith, T.; Al-Laham, M. A.; Peng, C. Y.; Nanayakkara, A.; Gonzalez, C.; Challacombe, M.; Gill, P. M. W.; Johnson, B.; Chen, W.; Wong, M. W.; Andres, J. L.; Gonzalez, C.; Head-Gordon, M.; Replogle, E. S.; Pople, J. A. *Gaussian 98*; Gaussian Inc.: Pittsburgh, PA, 1998.
(8) Jorgensen, W. L.; Chandrasekhar, J.; Madura, J. D.; Impey, R. W.; Klein, M. L. *J. Chem. Phys.* **1983**, *79*, 926−935.
(9) MacKerell, J. A. D.; Bashford, D.; Bellott, M.; Dunbrack, R. L., Jr.; Evanseck, J. D.; Field, M. J.; Fischer, S.; Gao, J.; Guo, H.; Ha, S.; Joseph-McCarthy, D.; Kuchnir, L.; Kuczera, K.; Lau, F. T. K.; Mattos, C.; Michnick, S.; Ngo, T.; Nguyen, D. T.; Prodhom, B.; Reiher, W. E., III.; Roux, B.; Schlenkrich, M.; Smith, J. C.; Stote, R.; Straub, J.; Watanabe, M.; Wiorkiewicz-Kuczera, J.; Yin, D.; Karplus, M. *J. Phys. Chem. B* **1998**, *102*, 3586.
(10) Verlet, L. *Phys. Rev.* **1967**, *169*, 98.
(11) Berendsen, H. J. C.; Postma, J. P. M.; Van Gunsteren, W. F.; DiNola, A.; Haak, J. R. *J. Chem. Phys.* **1984**, *81*, 3684.
(12) Harvey, S. C.; Tan, R. K.-Z.; Cheatham, T. E., III. *J. Comput. Chem.* **1998**, *19*, 72−740.

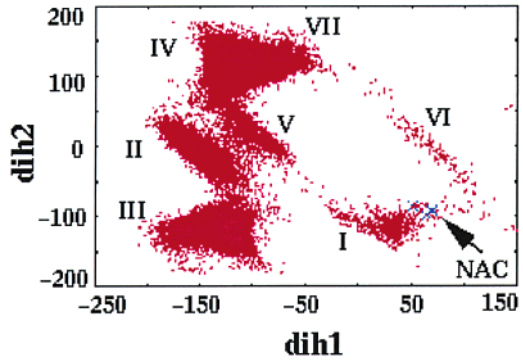

Figure 1. Plots of conformers on the conformational space of dih1 (C4−C3−O13−C14) vs dih2 (C3−O13−C14−C16). Conformers **I**−**VII** reside in distinguished areas of the conformational space. Less clear separation between **IV** and **VII** is due to sampling over a long period. NAC is a subspecies of conformer **I** and is marked with × (blue).

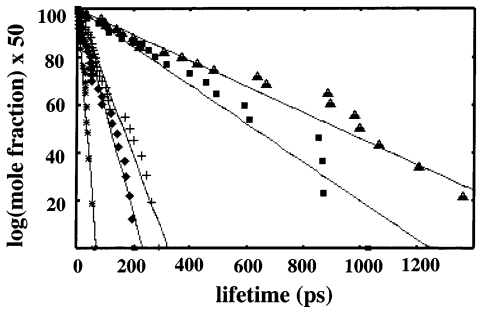

Figure 2. First-order kinetic plots of conformers **I** (◆), **II** (+), **III** (△), **IV** (□), and **V** (*). Data of **II**−**V** are taken from 10 ns and 20 ns simulations and data for **I** are from thirty additional simulations starting from **I**.

result validates sufficient sampling through the MD simulations. The slope of each linear fit corresponds to the first-order rate constant for disappearance of the conformer (k_{dis}). The k_{dis} of conformer **I** was not obtained from 10 and 20 ns MD simulations because it appeared only once. To obtain the needed statistics for disappearance of conformer **I**, additional thirty MD simulations were performed, starting from thirty geometries of the Boltzman distribution of conformer **I** (see Figure 1). Each system was energy minimized and heated to 300 K with constraints on dih1 and dih2 to keep the initial geometry. The constraints were released in 15 ps after the initiation of the simulation. The lifetime of conformer **I** was recorded after the total energy of the system reached the equilibrium (i.e., 65 ps after the release of the constraints). The same procedure was repeated for thirty systems of conformer **I** and the statistics of lifetime of conformer **I** were obtained. k_{dis} of conformer **I** was calculated from a plot of log(population) vs. lifetime (Figure 2).

MD Simulation of Chorismate Mutase Complexed with Transition State Analogue (TSA). A MD simulation of *endo*-oxabicyclic TSA (Chart 2) complexed to the EcCM was performed and the result was compared with the previously reported simulations of EcCM·CHOR and EcCM·TS.[6] Choice of a crystal structure[14] and protocols for a simulation were the same[6] as in the EcCM·CHOR and EcCM·TS simulations. The force fields for TSA were adopted from the modified MSI parameters and the standard CHARMM parameters (version 27) for the enzyme. The atomic charges for TSA were calculated by RESP (Restrained ElectroStatic Potential)[15] fitting to the potential generated at the MP2/aug-cc-pVDZ//B3LYP/6-31+G(d,p) level of theory using Merz−Kollman scheme.[16] The final system consisted of a dimeric EcCM with TSA's bound to each of the two active sites, contained in the 90 × 60 × 50 Å^3 box of 7599 TIP3P[8] water molecules. After 50 ps of heating, the simulation was continued in equilibrium state for 500 ps. The root-mean-square-deviation of the EcCM backbone remained less than 1.6 Å for the entire trajectories.

Results

Ground State Conformers of Chorismate in Water. Chorismate can be either in diaxial or in diequatorial configurations, depending on the dihedral angle of O10−C2−C3−O13. Only diaxial conformers can lead to the TS. Our force fields for dih1 (dihedral angle of C4−C3−O13−C14) and dih2 (C3−O13−C14−C16) of chorismate are designed for diaxial configurations. Throughout an MD simulation period of 33 ns (one 10 ns, one 20 ns, and thirty simulations for 0.1 ns), it was found that CHOR exists in seven diaxial conformers (**I**−**VII** in Figure 1). These conformers interchange from one to another by following certain paths (Chart 3). In the 10 and 20 ns MD simulations, the conformers **II**−**V** occur frequently (∼16 times). This allows one to estimate relative concentrations and first-order rate constants for disappearance of conformers **II**−**V**. A relative concentration of each conformer is calculated by the total fraction of time the chorismate resides as the conformer (Table 1). First-order rate constants for decomposition were obtained from the slopes of the plots of log(population) vslifetime (see Methods) (Figure 2). In general, a mole fraction of each conformer is a half-life (ln(2)/k_{dis}) multiplied by the probability of formation of the conformer. It was shown, in our simulation, that for **II**−**V** the log(mole fraction) and log(half-life) are linearly correlated with the correlation coefficient of 0.995 and the slope of 1.09 (Figure 3). Thus, the relative mole fraction of **II**−**V** is mainly determined by the duration period of these conformers, and the probability of formation is similar among them. Using this relationship, the mole fraction of any conformer can be estimated if k_{dis} and the frequency of formation relative to **II**−**V** were known. k_{dis} of conformer **I** was calculated from thirty additional simulations started from conformer **I** (see Methods). The linear fit equation in Figure 3 predicts that the mole fraction of **I** would be 14% if **I** occurs as frequently as **II**−**V**. Apparently formation of conformer **I** is more than 10 times less probable than formation of **II**−**V**. This is because, during the 10 ns and 20 ns MD trajectories, **I** never reappeared even when starting from **I**, whereas each of **II**−**V** occurs more than 15 times. Thus, supposing that the frequency of formation of **I** is 10 times less than those of **II**−**V**, the mole fraction of **I** would be 1.4%. The final mole fractions and k_{dis}'s of conformers are summarized in Table 1.

On the basis of their geometries the relative stabilities of conformers can be understood. Conformers **IV** and **III** are the most probable and disappear from solution most slowly. As can be seen in Chart 3, **IV** is stabilized by one water molecule bridging between the side chain carboxylate and the hydroxyl groups. Structure of **IV** is similar to one of the gas-phase diaxial conformers,[6] of which the same carboxylate forms an intramolecular hydrogen bond with H−C2. The structure **III** is not detected in the ab initio calculation in the gas phase, but the potential energy surface generated by molecular mechanics force

(13) When conformer A is changed into conformer B the transition is observe in the plots of dih1 and dih2 as functions of time. The time correponding to the midpoint of the transition is considered as a disappearing point of conformer A and an appearing point of B.
(14) Lee, A. Y.; Karplus, P. A.; Ganem, B.; Clardy, J. *J. Am. Chem. Soc.* **1995**, *117*, 3627−3628.
(15) Balyl, C. I.; Cieplak, P.; Cornell, W. D.; Kollman, P. A. *J. Phys. Chem.* **1993**, *97*, 10269−10280.
(16) Besler, B. H.; Merz, K. M.; Kollman, P. A. *J. Comput. Chem.* **1990**, *11*, 431−439.

Chart 3

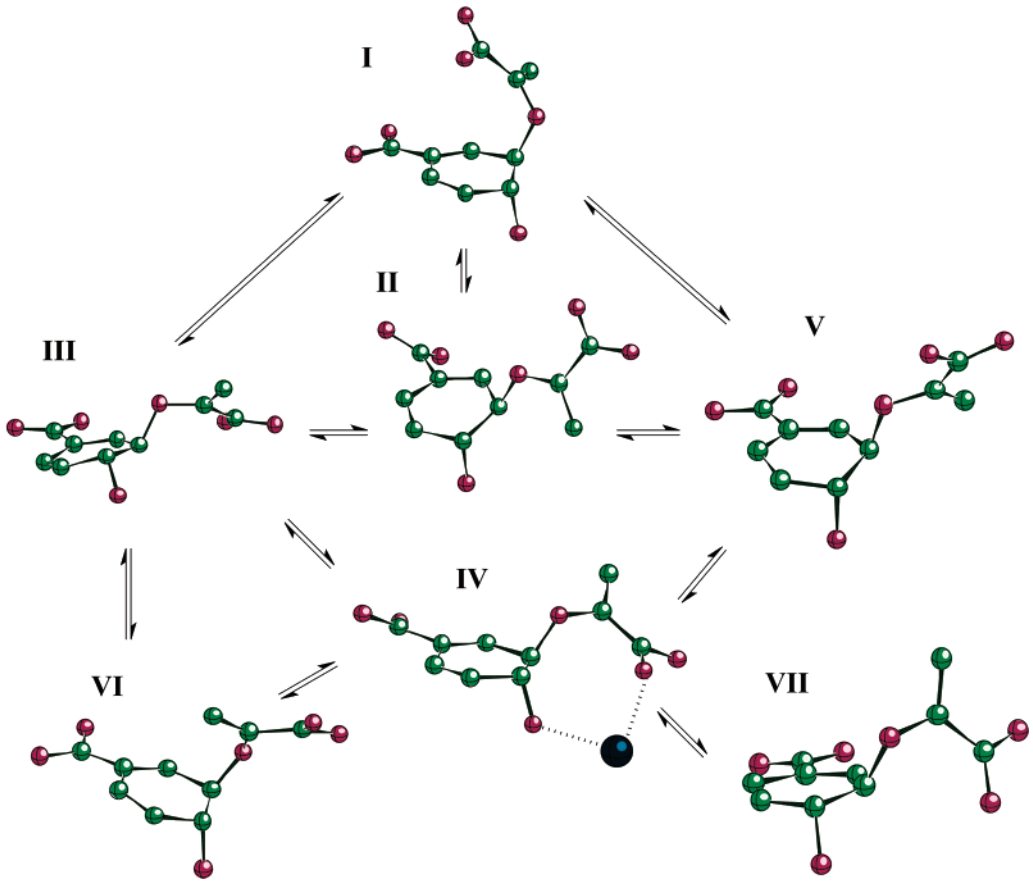

Table 1. Mole Fraction of Each Conformer Relative to the Total Diaxial Conformers and Dissociation Rate Constant k_{dis}

conformers	mole fraction (%)	$k_{dis} \times 10^9$ (s^{-1})
I	1.4	8.6
II	13	6.2
III	36	1.6
IV	48	1.1
V	2.3	30
VI	< 0.1	
VII	< 0.2	

The values for the conformer **II**−**VII** were obtained from 10 ns and 20ns simulations whereas values for **I** was calculated from 30 additional simulations.

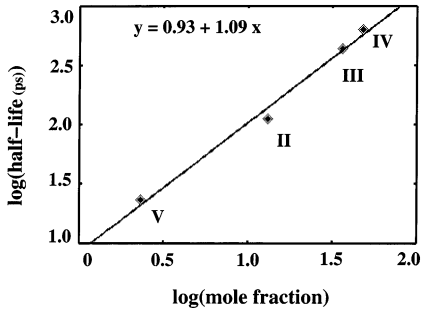

Figure 3. The linear relationship between log(half-life) and log(mole fraction). Each point is taken from the values in Table 1. The equation of the linear fit is shown on top.

fields in the gas phase with the charge−charge interaction energy term turned off showed **III** is favored by an intrinsic dihedral preference. Depending on the direction of dih1 and dih2 rotations, **III** and **IV** can be interchanged mainly in three different ways; directly, via **II** and **V**, or via **VI** (Chart 3). These five conformers **II**−**V** occur most frequently during the simulation.

Conformers **II**−**VII** all have the side chain carboxylate away from the ring moiety. The only conformer that has the carboxylate positioned above the ring is **I**. In these geometries, the distance between the two carboxylate oxygens ($COO^{-}\cdots{}^{-}OOC$) is >8 Å for **II**−**VII**, but is ∼4−7 Å for **I**. The early studies on substituent effects of dicarboxylic acids showed that the acid dissociation constants of the two carboxyl functions diverge as the two carboxylates are brought together.[17,18] In our simulation, **I** is present for 1.4% of the time. When two carboxylates are brought in proximity to the point where the hydration shells of the two carboxylates overlap ($COO^{-}\cdots{}^{-}OOC$ < ∼7 Å) as in **I**, water molecules rearrange themselves such that a water of one hydration shell is hydrogen bonded to another water in the other hydration shell (Chart 4). This maximizes the hydrogen bonding network and reduces the electrostatic repulsion between the two carboxylates. Because of this essential role of water in stabilizing **I**, conformer **I** is not found in the gas phase.

Mechanism of Formation of Near Attack Conformer (NAC) in Water. Near Attack Conformers (NACs) are defined as having the C5−C16 distance ≤3.7 Å and the attack angle ≤30° (Chart 1). To form a NAC the side chain carboxylate must be positioned above the ring moiety. Among the seven conformers, only **I** can directly form a NAC. **I** exists with two distinguishable water structures (**Ia** and **Ib**), depending on the $COO^{-}\cdots{}^{-}OOC$ distance (Chart 5). When the $COO^{-}\cdots{}^{-}OOC$

(17) Kirkwood, J. G.; Westheimer, F. H. *J. Chem. Phys.* **1938**, *6*, 506−513.
(18) Bruice, T. C.; Bradbury, W. C. *J. Am. Chem. Soc.* **1965**, *87*, 4851−4855.

Chart 4

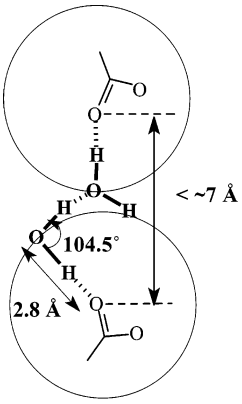

Ib

distance < ~5 Å, a water molecule directly bridges between two carboxylates (**Ia**). When ~5 Å < $COO^-\cdots{}^-OOC$ < 6 Å, the two carboxylates cannot be directly bridged via one water molecule, but it is possible via two water molecules (**Ib**). **Ia** and **Ib** interchange frequently by a swing motion of the side chain. This is seen from the anti-correlation between the C5−C16 distance and the $COO^-\cdots{}^-OOC$ distance (Figure 4). When the $COO^-\cdots{}^-OOC$ distance becomes longer the C5−C16 distance decreases and when the $COO^-\cdots{}^-OOC$ becomes shorter the C5−C16 distance increases. NAC is formed during a time period of 60−80 ps in Figure 4 when the $COO^-\cdots{}^-OOC$ distance is within 6−7 Å. At this distance, the two carboxylates of NAC are not hydrogen bonded via water molecules although two hydration shells remain in overlap. The side chain carboxylate of NAC is positioned right above the ring. The instability of NAC may be due to the hydration shell of the carboxylate being distorted by steric conflict with the ring (Figure 5). Also the effect from electrostatic repulsion between the carboxyl functions might increase in NAC structure due to the lack of stabilizing force provided by the hydrogen bonds between waters solvating the two carobxylates. Out of the thirty simulations of conformer **I** for the total period of 2.3 ns, NAC exists for 0.05% of the time of conformer **I**, which corresponds to 0.0007% of the time of total diaxial conformers. NMR measurements showed that the mole fraction of diaxial conformers relative to the total ground state is ~10% in water.[19] Thus, the mole fraction of NAC relative to the total ground state is 0.000 07%.

TSA Simulation. The interaction between an enzyme and a ligand bound at the active site can be studied by an MD simulation of the enzyme·ligand complex. An MD simulation of chorismate mutase (EcCM) complexed with the *endo*-oxabicyclic transition state analogue (TSA, Chart 2)[4] was carried out for 500 ps, and the results were compared with the previously reported[6] MD simulations of the chorismate-bound EcCM (EcCM·CHOR) and the TS-bound EcCM (EcCM·TS). Table 2 and Chart 6 summarizes the interaction distances between EcCM and CHOR, TS or TSA. The interactions between the EcCM and ligands are divided into electrostatic and hydrophobic interactions (Chart 6). It can be clearly seen that the electrostatic interactions at the ligand carboxylate groups (a−d), which fix the ligand at the active site do not vary among EcCM·CHOR, EcCM·TS, and EcCM·TSA. When superimposing the enzyme backbones of EcCM·CHOR, EcCM·TS, and EcCM·TSA, the positions of the ligand carboxylates match very well. The geometry of the ligand changes in bond-breaking and bond-making positions. Electrostatic residues interacting with bond-breaking ether oxygen (O13) are Lys39 and Gln88. These residues are flexible and accommodate their terminal functions as the ligand changes. The length of the breaking bond C3−O13 is longer in TS (2.24 Å) than in CHOR and TSA (1.42 Å), but the interaction distances at O13 from Lys39(NZ) and Gln88(NE2) differ only by less than 0.2 Å. Interactions at the forming bond C5−C16, however, vary according to the type of the ligand bound to the enzyme. Val35 and Ile81, which form hydrophobic contact with CHOR's C16 and C5, respectively, are not in contact with those atoms of the TS or TSA (Figure 6). The change in the hydrophobic interaction distances are as follows; C16···Val35: CHOR (3.65 Å) < TS (4.06 Å) < TSA (5.00 Å); C5···Ile81: CHOR (3.83 Å) < TS (4.44 Å) < TSA (5.73 Å). Superposition of the three structures shows little change in the positioning of Val35 and Ile81. The change in the interaction distance is a reflection of the size of the ligand as measured by the C5−C16 distance: CHOR (3.65 Å on average) > TS (2.58 Å) > TSA (1.52 Å). The hydrophobic chain of Arg51 forms a broad van der Waals contact with the ring moiety (C1 and C6). The interaction distance is similar in EcCM·CHOR and EcCM·TSA, but ~0.5 Å longer in the EcCM·TS. This might be due to the more polar character of the TS compared to CHOR or TSA.

Discussion

Importance of Formation of Near Attack Conformer (NAC) in the Chorismate → Prephenate Reaction. Near attack conformers (NACs) are ground state conformers which must be formed in order that a reactant can enter the TS of a reaction. The kinetic importance of NAC formation in the chorismate → prephenate reaction (Chart 1) in water and when catalyzed by the *E. coli* chorismate mutase (EcCM) has been determined by use of a number of MD simulations. Heavy atom kinetic isotope effects show that the C5−C16 bond formation and the C3−O13 bond cleavage are concerted as in other pericyclic reactions in both water and the enzyme reactions.[20] Although the bond cleavage is more pronounced in both reactions, the CHOR side chain C16 must be positioned above C5 in a chairlike configuration in order to reach the TS. We define NAC as a conformer having the C5···C16 distance ≤3.7 Å and the attack angle ≤30° in a chairlike geometry (Chart 1).

In our simulations, NAC occurs 0.000 07% of the time in water and 32% of the time at the EcCM active site.[6] This shows that NAC formation is more facile at the active site by 7.8 kcal/mol compared to its formation in water (Chart 7). The experimentally measured rate enhancement on going from water to the enzyme is 10^6 fold,[21] which corresponds to lowering of the activation barrier by ~9 kcal/mol. Thus, *EcCM* gains ~87 % of its kinetic advantage over the water reaction by enhancing NAC formation at the active site.

Formation of NAC also prevents other side reactions from occurring. Chorismate also undergoes an elimination reaction

(19) Copley, S. D.; Knowles, J. R. *J. Am. Chem. Soc.* **1987**, *109*, 5008−5013.

(20) Gustin, D. J.; Mattei, P.; Kast, P.; Wiest, O.; Lee, L.; Cleland, W. W.; Hilvert, D. *J. Am. Chem. Soc.* **1999**, *121*, 1756−1757.

(21) Chook, Y. M.; Gray, J. V.; Ke, H.; Lipscomb, W. N. *J. Mol. Biol.* **1994**, *240*, 476−500.

Chart 5

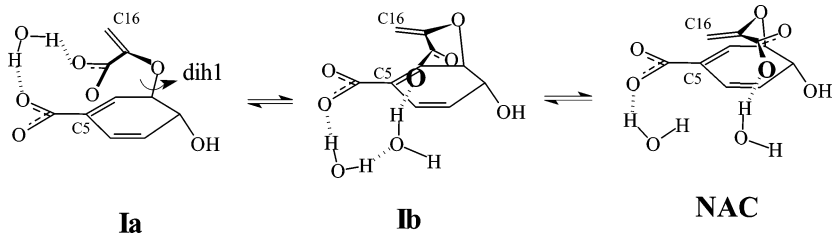

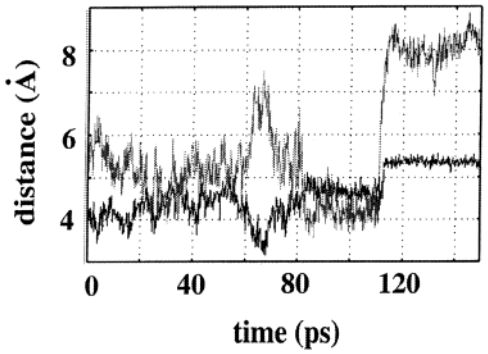

Figure 4. Plot of the C5··C16 distance (black) and the −COO⁻···⁻OOC− distance (gray) as functions of time. From a time period of 0−110 ps, chorismate is in conformer **I**. After 110 ps, chorismate is in the conformer **II**. During the 0−110 ps, the two distances are anti-correlated. NAC is formed in the time range of 60−80 ps, when the −COO⁻···⁻OOC− distance is > ∼7 Å and the C5···C16 distance is <3.7 Å.

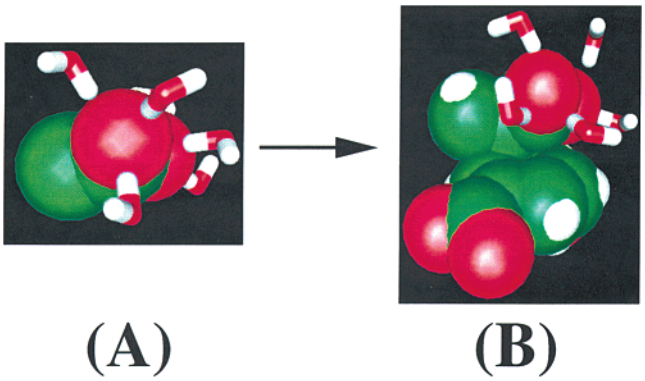

Figure 5. First hydration shell (the COO⁻···HOH distance <2.4 Å) of the side chain carboxylate, (**A**) when away from the ring and (**B**) when positioned above the ring of CHOR. In (**B**) water molecules near the ring are arranged such that H−O−H lies parallel to the ring moiety.

of the ether vinyl side chain in the same water environment at ∼50% of the rate of the Claisen rearrangement.[22] The elimination reaction does not occur in the active site.[23] This is because the NAC for the Claisen rearrangement cannot lead to the TS in the elimination reaction. The TS involved in the elimination reaction has the side chain C16 near C2 while the TS in the Claisen rearrangement has C16 in proximity of C5.[22]

Mechanism of NAC Formation in Water and in Enzyme. In our MD simulation of chorismate in water, seven diaxial conformers were identified (**I**−**VII** in Chart 3). By observing the motion of each conformer throughout a total of 33 ns trajectory, we have derived the kinetic as well as thermodynamic properties of these conformers (Table 1). All of the conformers **II**−**VII** (∼99%), except for **I**, commonly involve the side chain carboxylate away from the ring moiety. This propensity is due to the repulsive interaction between the two carboxylate substituents as characterized by Westheimer and Kirwood[17] and further studied by Bradbury and Bruice.[18] Only conformer **I** has the two carboxylates in proximity and only **I** is capable of forming a NAC. In this geometry of **I**, the water shells hydrating the two carboxylates overlap. To reduce the electrostatic repulsion, the water molecules in the overlap region arrange themselves to form bridging hydrogen bonds between the two carboxylates (Chart 4). The water structure of **I** has been previously identified by QM/MM and ab initio studies.[24] It has been observed that the chorismate → prephenate reaction rate drops by 100 fold when transferred from water to methanol.[19] This may be due to the loss of solvent ability in stabilizing conformer **I**.

Depending on the distance between the two carboxylates, two configurations of water structure (**Ia** and **Ib**) were found (Chart 5). In **Ia**, two carboxylates are directly bridged by one water molecule, whereas in **Ib**, two water molecules are involved in the bridging hydrogen bonds. NAC is formed from **Ib** by a rotational fluctuation of the side chain around dih1 (Chart 5). NAC remains for less than 1 ps. During the period of NAC formation, the bridging hydrogen bonds between the two carboxylates are broken and the side chain carboxylate is positioned right above the hydrophobic ring moiety (Figure 5). Fluctuation of **Ib** into NAC is not favored due to the steric conflict between the ring and the hydration shell of the side chain carboxylate along with loss of water-mediated hydrogen bonds.

At the active site of EcCM, the two carboxylates are tightly held by adjoining with Arg28 and Arg11* of neighboring subunits, respectively (Chart 6A). Formation of these salt bridges resolves the problem of electrostatic repulsion between the two carboxylates, which occurs in water and in the gas phase when forming NAC. Arg28 and Arg11* are tightly held by other auxiliary residues such that there is little fluctuation (0.23 Å) in the −COO⁻···⁻COO− distance of the bound CHOR. Being tightly held by two arginines, C16 is placed right under the Val35 methyl group and C5 is above the Ile81 terminal methyl group in the EcCM·CHOR complex (Figure 6A). Val35 and Ile81 increase the population of NAC at the active site by restricting other motions of C5 and C16. The effects from these hydrophobic crowdings do not involve a strain because there is no direct pushing from Val35 or Ile81 to C16 or C5.[6]

Comparison of Enzyme Binding Affinities with CHOR, TS, and TSA. The rate enhancement by chorismate mutase has been often explained by preferential interaction of enzyme with the TS compared to with CHOR. This was supported by the experimental measurements in which TSA binds ∼100 fold tighter than CHOR in water.[4] From the analysis of our MD

(22) Gajewski, J. J.; Jurayj, J.; Kimbrough, D. R.; Gande, M. E.; Ganem, B.; Carpenter, B. K. *J. Am. Chem. Soc.* **1987**, *109*, 1170−1186.
(23) Rajagopalan, J. S.; Taylor, K. M.; Jaffe, E. K. *Biochemistry* **1993**, *32*, 3965−3972.
(24) Guo, H.; Cui, Q.; Lipscomb, W. N.; Karplus, M. *Proc. Natl. Acad. Sci. U.S.A.* **2001**, *98*, 9032−9037.

Table 2. Average Interaction Distances (Å) between EcCM and Ligand

	protein residue	d(residue atom-ligand atom)	EcCM·CHOR	EcCM·TS	EcCM·TSA	
electrostatic interaction	Arg11[a]	(NE)−O18	**a**	2.69 ± 0.09	2.72 ± 0.10	2.73 ± 0.10
		(NH2)−O17	**a′**	2.67 ± 0.12	2.67 ± 0.10	2.67 ± 0.10
	Arg28	(NH1)−O23	**b**	2.66 ± 0.08	2.67 ± 0.08	2.65 ± 0.08
		(NH2)−O24	**b′**	2.72 ± 0.11	2.69 ± 0.09	2.75 ± 0.11
	Ser84	(OG)−O23	**c**	2.69 ± 0.11	2.72 ± 0.14	2.69 ± 0.14
	Asp48	(N)−O10	**d**	2.80 ± 0.16	2.75 ± 0.14	2.74 ± 0.10
	Lys39	(NZ)−O13	**e**	3.08 ± 0.19	2.82 ± 0.17	2.95 ± 0.18
	Gln88	(NE2)−O13	**f**	2.89 ± 0.15	2.86 ± 0.16	2.85 ± 0.15
hydrophobic interaction	Val35	(CG1)−C16	**g**	3.65 ± 0.20	4.06 ± 0.26	5.00 ± 0.33
	Ile81	(X)−C5	**h**	3.83 ± 0.36	4.44 ± 0.38	5.73 ± 1.06
	Arg51	(CG)−C1	**i**	3.75 ± 0.23	4.27 ± 0.28	3.81 ± 0.25

Values for EcCM·CHOR and EcCM·TS are obtained from the previous study (ref 6) and EcCM·TSA are from the current study. [a] Refers to the residue from the other subunit of the enzyme. [a] X = CD for EcCM·CHOR and EcCM·TSA, and X = CG2 for EcCM·TS.

Chart 6

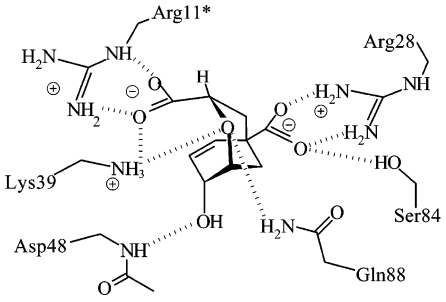

A. Electrostatic Interaction

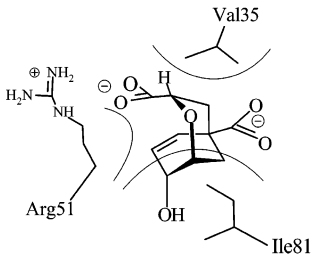

B. Hydrophobic Interaction

* refers to the residue from the other subunit of the enzyme

simulations, the 100 fold preferential binding of TSA relative to CHOR could not be attributed to preferential interaction of the enzyme with TSA as compared to the enzyme bound CHOR. The electrostatic interaction in the EcCM·TSA is comparable to that in the EcCM·CHOR, whereas hydrophobic interaction is stronger in the EcCM·CHOR than in the EcCM·TSA (Table 1). The protein Val35 and Ile81 do not change their positions when the larger CHOR (by measure of the C5··C16 distance) is substituted by the smaller TSA, in which case an empty space between the enzyme and TSA is created (Figure 6). The 100 fold tighter binding of TSA relative to CHOR can be ascribed to the free energy cost in bringing two carboxylates of CHOR to interact with the guanidine groups of Arg28 and Arg11*. The two carboxylates of TSA are fixed by a bicyclic structure at a distance of the two arginine functions (Chart 2), but this is not so for CHOR conformers **I**−**VII** in water. Comparison of binding affinities of series of inhibitors, which vary in the distance between two carboxylates, showed that the $COO^{-}\cdots{}^{-}OOC$ distance is essential for binding affinity.[4]

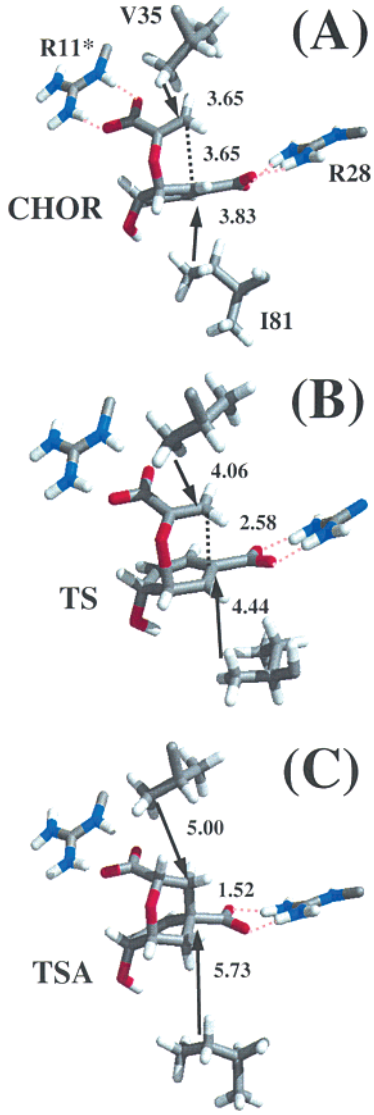

Figure 6. The active site of EcCM bound with (**A**) CHOR, (**B**) the TS and (**C**) TSA. The three distances (Å) shown in each panel are Val35(Cg)···C16, C16···C5, and C5···Ile81(Cd) distances, from the top to bottom.

Our previous MD simulations of EcCM·CHOR and EcCM·TS[6] also reveal that, in terms of interaction distances, the enzyme interacts with the TS no more strongly than with CHOR.

Chart 7

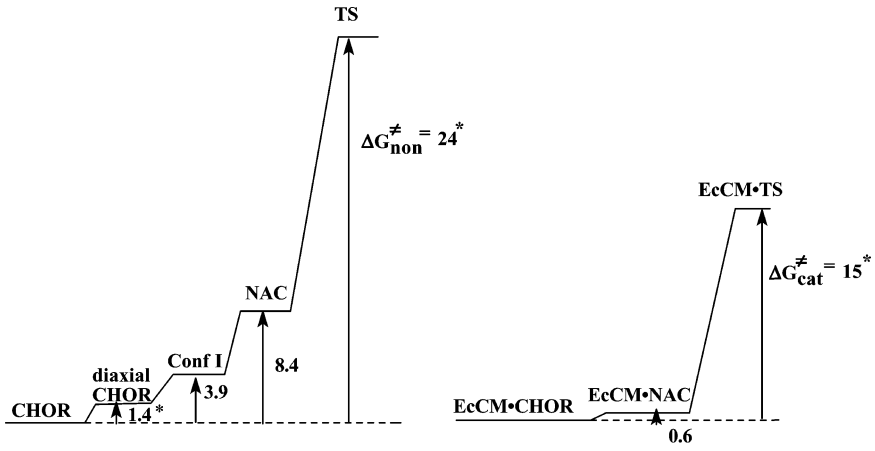

* : taken from experimental values (kcal/mol)

(A) uncatalyzed reaction **(B) catalyzed reaction**

Hydrophobic interactions become rather looser in the EcCM·TS than in the EcCM·CHOR and electrostatic interaction distances are comparable in both complexes. One might expect the charge development at the ether O13 in the TS may significantly affect the relative interaction energies. The ether O13 interacts with the protonated amino group of Lys39 and the amine of Gln88 (Chart 6A).[20,25] However, similar kinetic isotope effects at O13 in water and the enzyme reactions suggest[26] that the bond-cleavages are progressed to a similar extent in both reactions, and accordingly, the charge developments at O13 would be also similar in the TS of both the water and the enzyme reactions. An earlier computational study on the Claisen rearrangement of allyl vinyl ether showed that preferential stabilization of the TS ether O13 over the ground state is also present in the water reaction.[27] This was attributed to partial charge development and better solvent accessibility of O13 as the C3−O13 bond elongates in the TS in water. Considering all of these together, the preferential stabilization of O13 in the TS over ground state probably would be present, but does not appear to be significantly greater at the active site compared to in water. The reaction coordinates in Chart 7, constructed by experimental data and results from our simulations of ground state in water and in the enzyme, suggest that the TS stabilization by Lys39 (or Gln88) would be ∼1 kcal/mol than in water, which is a preferential stabilization of the TS compared to NAC.[28] This is 13% of $\Delta\Delta G^{\ddagger}$, where the other 87% is explained by the efficiency of the enzyme in forming NACs.

Conclusion

In this paper, we have described the ground state features of chorismate (CHOR) in water and determined the probability and mechanism of forming the reactive conformer (near attack conformer: NAC) for the noncatalyzed Claisen rearrangement (Chart 1). This was done by analyzing a number of molecular dynamics simulations of CHOR in water. This, along with our results from the previously reported simulation of *E. coli* chorismate mutase (EcCM) complexed with CHOR,[6] allowed us to reconstruct the reaction coordinates of the water reaction and the enzymatic reaction, in which ground state (GS) and transition state (TS) effects can be distinguished. The results show that, out of the 9 kcal/mol reduction in the reaction barrier of the enzymatic reaction compared to the water reaction, ∼90% is due to the efficiency of the enzyme in NAC formation compared to water (free energy cost for GS → NAC is 8.4 kcal/mol in water and 0.6 kcal/mol at the active site). The remained ∼10% is attributed to stabilization of the ether O13 by the protonated Lys39 (free energy cost for NAC → TS is 15.6 kcal/mol in water and 14.4 kcal/mol at the active site). Thus, the free energy of activation in the enzymatic reaction is almost the same as the free energy difference between NAC and the TS in water.

Chart 8

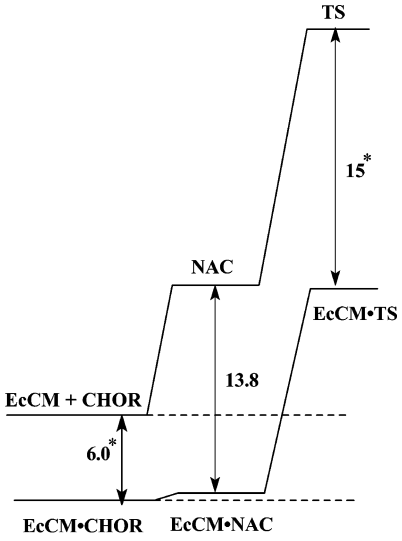

* : taken from experimental values

Viewing from a different point, the two reaction coordinates in Chart 7 were superimposed by use of the experimental value of K_m (Chart 8). The most of the enzyme proficiency, defined

(25) Liu, D. R.; Cload, S. T.; Pastor, R. M.; Schultz, P. G. *J. Am. Chem. Soc.* **1996**, *118*, 1789−1790.
(26) Personal communication with Cleland, W. W.
(27) Cramer, C. J.; Truhlar, D. G. *J. Am. Chem. Soc.* **1992**, *114*, 8794−8799.
(28) The free energy cost in NAC → TS in water is 15.6 kcal/mol whereas it is 14.4 kcal/mol at the enzyme. It follows that TS stabilization relative to NAC due to its charge distribution accounts 1.2 kcal/mol among total $\Delta\Delta G^{\ddagger}$, 9 kcal/mol.

by Wolfenden[29] as a free energy difference of the TS in water and the enzyme (15 kcal/mol), comes from the stabilization of the ground state NAC (13.8 kcal/mol). NAC as well as TS are very unstable species in water, due to (i) the electrostatic repulsion between the two carboxylates and (ii) the steric conflict between the hydration shell of the side chain carboxylate and the ring. These problems are resolved at the active site by conjugating the two carboxylates with the fixed Arg28 of one subunit and Arg11* of the other subunit of the enzyme. Because of the similar geometrical nature of ground state NAC and the TS, stabilization of ground state NAC compares with the stabilization of the TS. The additional stabilization (1.2 kcal/mol) of the TS relative to NAC can only be achieved by the difference in the charge distribution at the bond-breaking site. This is done by the Lys39···O13 interaction. Although the absolute stabilization of the TS ether O13 relative to the NAC may be substantial, this preferential stabilization by Lys39 at the active site in excess of water stabilization does not appear to be significant (∼1 kcal/mol), according to Chart 8.

(29) Wolfenden, R.; Snider, M. J. *Acc. Chem. Res.* **2001**, *34*, 938−945.

Currently there is no experimental means to distinguish between GS and TS effects, since free energy of NAC formation in water and in the enzyme is difficult to determine experimentally. K_d of transition state analogue (TSA) and K_m are often used as indirect measures of these effects. From our simulation of EcCM·TSA and EcCM·CHOR, it was shown that experimentally measured ∼100 fold tighter binding of TSA relative to CHOR does not originate from preferential interaction of TSA compared to the enzyme bound CHOR. The tighter binding of TSA originates from the free energy cost of bringing the two carboxylates of CHOR into the preferable position for binding, whereas the carboxylates of TSA are fixed by the rigid bicyclic structure.

Acknowledgment. This study was supported by a grant from National Science Foundation (MCB-9727937) and Provost funds, University of California, Santa Barbara. The authors gratefully acknowledge computer time on the University of California, Santa Barbara SGI Origin2000 and at the NPACI (San Diego Supercomputer Center).

JA0210648